PHYSICAL REVIEW A **69**, 011802(R) (2004)

Laser spectroscopy of hydrogenlike nitrogen in an electron beam ion trap

K. Hosaka, D. N. Crosby, K. Gaarde-Widdowson, C. J. Smith, and J. D. Silver
Department of Physics, University of Oxford, Oxford OX1 3PU, United Kingdom

T. Kinugawa and S. Ohtani
Cold Trapped Ions Project, JST, University of Electro Communications, Chofu, Tokyo 182-0024, Japan

E. G. Myers
Department of Physics, Florida State University, Tallahassee, Florida 32306, USA

(Received 3 October 2003; published 30 January 2004)

Using a $^{14}C^{16}O_2$ laser the $2s_{1/2}$-$2p_{3/2}$ (fine structure–Lamb shift) transition has been induced in $^{14}N^{6+}$ ions trapped in an electron beam ion trap. The transition has been measured to be 835.0 ± 0.5 cm^{-1}, in agreement with QED theory.

DOI: 10.1103/PhysRevA.69.011802 PACS number(s): 42.62.Fi, 39.30.+w, 12.20.Fv

Laser spectroscopy of few-electron highly charged ions [1,2] can produce precise tests of modern, relativistic atomic theory [3–6]. The usual technique for producing the highly charged ions is to foil strip an accelerated ion beam at $v/c \approx 0.1$. For example, fast-beam laser spectroscopy has been carried out at energies of a few MeV/nucleon to test Lamb shift calculations in hydrogenlike N^{6+} [7], F^{8+} [8], P^{14+} [9,10], S^{15+} [11], and Cl^{16+} [12], and also to test calculations of fine structure in heliumlike ions [2,13]. Laser spectroscopy of the ground-state hyperfine structure of hydrogenlike $^{209}Bi^{82+}$ [14] and $^{207}Pb^{81+}$ [15] has been carried out with 200-MeV/nucleon beams in a heavy-ion storage ring.

By using copropagating and counterpropagating laser beams in fast-beam spectroscopy the uncertainty due to the Doppler shift can be greatly reduced, and sub-part-per-10^6 precision for energy intervals in highly charged ions has been achieved [16]. However, it seems that the precision of such fast-beam methods will be ultimately limited by the Doppler shift combined with laser wave-front curvature effects. Hence there is considerable interest in developing techniques for laser spectroscopy on highly charged ions in ion traps, where there is no net center-of-mass motion and no overall Doppler shift.

The electron beam ion trap (EBIT) [17] uses a magnetically compressed electron beam to produce and trap highly charged ions. In one development it has produced fully stripped uranium [18]. It has been used extensively for emission spectroscopy in the x-ray, UV, and visible regions of the spectrum. Laser spectroscopy of the Lamb shift of hydrogenlike ions in an EBIT has been previously proposed and studied [19], and an attempt at laser spectroscopy of magnetic-dipole transitions between fine-structure components of the ground state of Ar^{10+} in an EBIT was made [20]. Highly charged ions have been transferred from an EBIT to a secondary Penning trap, and then sympathetically cooled using laser-cooled Be^+ ion [21], also with the aim of laser spectroscopy of magnetic-dipole transitions in the highly charged ions [22,23]. Here we report the observation of a resonant increase in the yield of x rays from decay of the $2p_{3/2}$ level of N^{6+} ions in an EBIT, due to irradiation with laser light at wavelengths near 12.0 μm, corresponding to the $2s_{1/2}$-$2p_{3/2}$ (fine structure–Lamb shift) transition [7,24,25]. To our knowledge, this is the first report of laser spectroscopy of highly charged ions in an EBIT.

The relevant energy levels of N^{6+} are shown in Fig. 1. The principle of the experiment is that the laser induces the transition from the metastable $2s_{1/2}$ level, mean lifetime 1.03 μs [26,27], to the $2p_{3/2}$ level, mean lifetime 0.66 ps [28]. The $2s_{1/2}$ level usually decays emitting two photons whose sum energy is 500.3 eV, while the $2p_{3/2}$ level decays emitting the Lyman-α x ray at 500.4 eV. Hence the transition is detected as an increase in the yield of x rays at 500 eV, or as a reduction in yield of the two-photon x rays, whose continuous spectrum has the maximum at 250 eV. A schematic diagram of the experimental setup is shown in Fig. 2. In the Oxford EBIT [29], a 1.5 keV, 30 mA, vertical electron beam was compressed to about 70 μm in diameter by the 3-T magnetic field produced by a pair of superconducting Helmholtz coils. Voltages applied to a series of three ''drift tubes'' centered between the coils provided the axial potential well to confine the ions. The drift-tube structure was maintained at liquid He temperature and was enclosed inside the magnet structure, also at liquid He temperature, except for eight 16-mm diameter openings for spectroscopic access. The base vacuum, measured outside a surrounding liquid N_2 shield, was 4×10^{-10} mbar. The central drift tube, of vertical length 31 mm, has eight vertical slots 2.5-mm wide and 25-mm

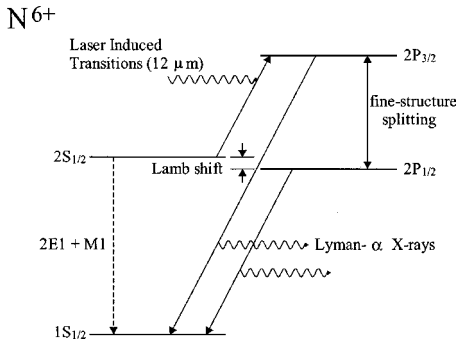

FIG. 1. Schematic energy level diagram of hydrogenlike nitrogen showing the laser-induced transition.

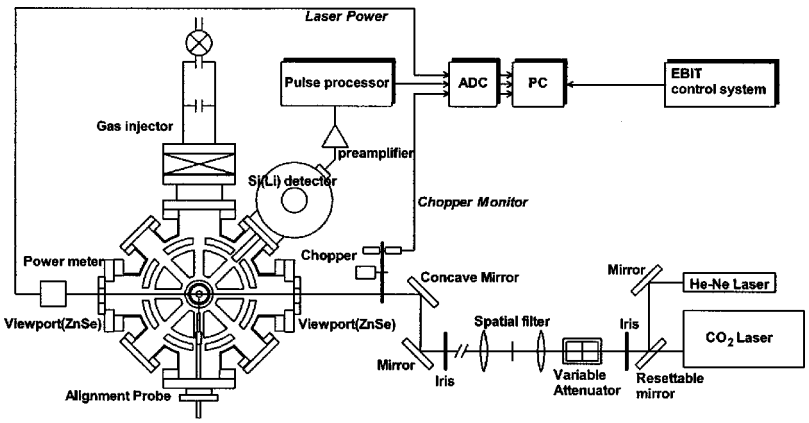

FIG. 2. Schematic diagram of the apparatus used for a measurement of the $2s_{1/2}$-$2p_{3/2}$ transition frequency in hydrogenlike N^{6+}. The electron beam in the EBIT is directed out of the page.

long. Nitrogen gas injected from outside the EBIT passed as a molecular beam through one of these slots, perpendicular to the electron beam, at a typical rate of 5×10^9 molecules s^{-1}. Electron impact dissociates and ionizes some of the nitrogen molecules. The resulting ions are trapped radially by the space charge of the electron beam, and axially by biasing the central drift tube 50 V relative to the outer tubes. Sequential impact by electrons in the beam produces highly charged ions. To limit build-up in the trap of highly charged barium and other ions sputtered from the electron-beam cathode, the ion trap is periodically emptied for about 100 ms following a trapping time of 2 s.

In this experiment, the Lyman-α x rays from excited ions were detected using a 30 mm^2 Si(Li) detector, fitted with a thin aluminized polymer window [30], which viewed the trapped ion cloud through another slot in the central drift tube. The estimated quantum efficiency of the Si(Li) detector was 45% at the N^{6+} Lyman-α energy of 500.4 eV. A collimator in front of the detector restricted the region of the ion cloud viewed to a 4 mm vertical length in the center of the drift tube, with an average detection solid angle of 5.3 msr. After optimization of the N_2 gas injection the average x-ray count rate, in the region of the Si(Li) detector spectrum corresponding to the N^{6+} Lyman-α x rays, was about 2500 counts per second, see Fig. 3(a). The background consists of other K x rays from N^{6+} and in N^{5+}, and of L x rays from higher-Z contaminant ions. By fitting the data in Fig. 3(a) this x-ray background is estimated to contain 60% of x rays from Lyman-α.

The laser was a grating-tuned carbon-dioxide laser with sealed-off tubes containing $^{14}C^{16}O_2$. To scan over the resonance, which has a natural width of 8.0 cm^{-1} [28], the laser was manually tuned from the P-24 to the P-42 lines of the P branch of the $[00^01]$-$[100^00, 02^00]$ vibrational-rotational transition [31]. Because of the variation in the laser gain, the maximum laser output fell from 28 W to 5 W, at the long wavelength end of the range. To ensure a near constant power and intensity entering the EBIT use was made of a spatial filter, and also a variable attenuator consisting of a pair of rotatable ZnSe plates. The laser beam, which was vertically polarized, was focused using off-axis reflection from a concave mirror, entered the EBIT through a ZnSe window with transmission of 97%, and was directed through another slot in the central drift tube, intersecting the electron beam at right angles. At this intersection, which was centered at the region viewed by the Si(Li) detector, the laser spot size was approximately 1.7-mm wide and 3.8-mm high. The laser beam was chopped at 125 Hz with a 50% duty cycle by a chopper wheel, and the power transmitted through the EBIT was measured with a power meter on the opposite side. The pulse-height analyzed Si(Li) signal was fed to a PC along with a synchronization signal from the chopper, together with the laser power reading. A He-Ne laser and a retractable probe in the side of the EBIT were used to align the CO_2

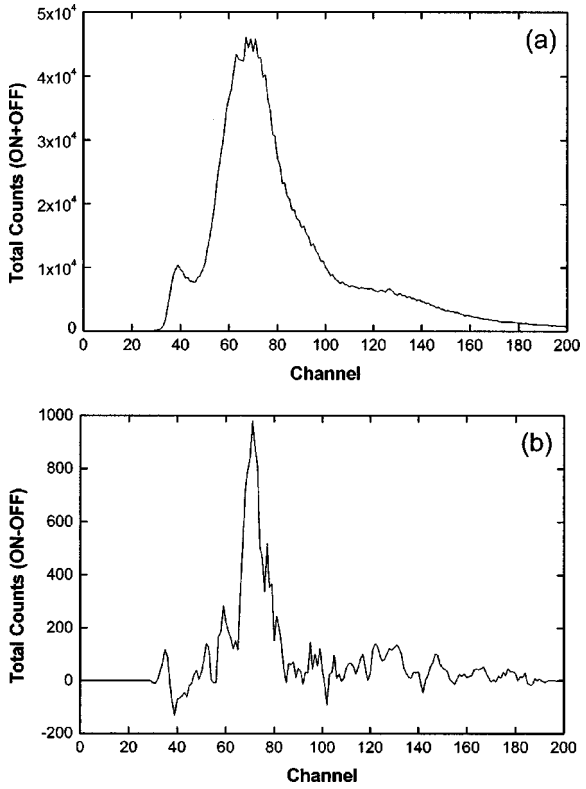

FIG. 3. Enhancement of the x-ray emission from hydrogenlike N^{6+} ions induced by laser interaction as a function of the x-ray energy. (The channel number is roughly proportional to pulse height and x-ray energy.) (a) shows the total x-ray counts, while (b) shows the laser-induced signal, namely, x-ray counts (laser on)–x-ray counts (laser off). These spectra were recorded in a total time of 500 s.

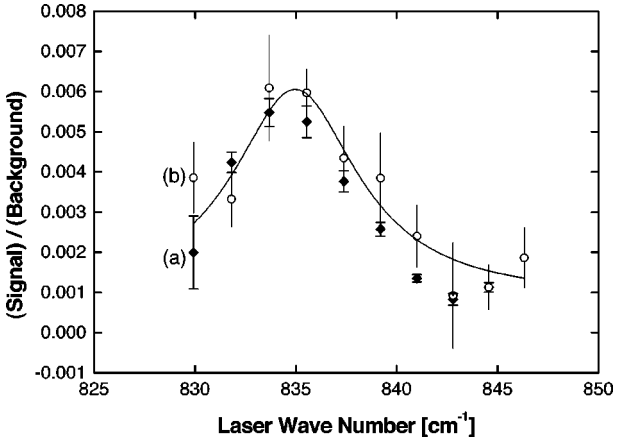

FIG. 4. The $2s_{1/2}$-$2p_{3/2}$ resonance in hydrogenlike N^{6+} obtained by changing the laser wave number [(a) solid] without the laser power leveled, and [(b) open] with the laser power leveled to 4.9 $\pm$0.3 W. For (b), the y scale shows the fractional increase in x rays in the energy range corresponding to Lyman-α. The data in (a) have been normalized to the same power for comparison. The curve is a Lorentzian fit to the power leveled data (b).

laser to the electron beam.

The enhancement of x rays from hydrogenlike N^{6+} ions induced by laser interaction is clearly observed in the x-ray spectrum obtained with the Si(Li) detector is shown in Fig. 3(b). For this measurement, the laser wavelength was fixed on the $P36$ laser line of $^{14}C^{16}O_2$ (835.537 cm^{-1}) with a spatially averaged power density of 3.5 W/mm^2. The laser-induced signal in Fig. 3(b) was obtained by subtracting the x-ray count obtained with the laser blocked by the chopper wheel from the x-ray count with the laser entering the EBIT trapping region. The peak at around channel 70 in Fig. 3(b) corresponds to an enhancement of N^{6+} Lyman-α radiation due to the laser excitation. It is narrower than the peak in Fig. 3(a), which also contains x rays from N^{5+}, and states in N^{6+} with $n>2$, as well as from the two-photon decay of the N^{6+} $2s$ state.

The wavelength dependence of the laser-induced signal is shown in Fig. 4. Data were initially taken without the laser power being leveled. A clear resonance was observed, but whose centroid is shifted by effects of saturation and normalization of the laser power [Fig. 4(a)]. The experiment was then repeated with the laser power leveled to the weakest line using the variable attenuator and more careful alignment. This reduced the laser power to 4.9$\pm$0.3 W corresponding to an average laser intensity of 1.15$\pm$0.07 W/mm^2, with consequent reduction in the signal, see Fig. 4(b). Each point represents the average of seven to eight measurements, each requiring a time of 500 s, and the data were taken over a period of 4 days. A Lorentzian fit to the resonance obtained with leveled laser power gives a centroid of 835.0 cm^{-1} with a fit error of 0.5 cm^{-1} and the full width at half maximum of 7.6 cm^{-1} with a fit error of 2.5 cm^{-1}.

The fractional change $\Delta\Gamma/\Gamma$ in the Lyman-α count rate due to the laser-induced $2s_{1/2}$-$2p_{3/2}$ transition on resonance may be estimated using time-dependent perturbation theory and rate equations. In the EBIT the $2s$ and $2p$ levels are continuously populated by electron impact within the ion-laser interaction region. If the rates of formation of hydrogenlike ions in the $2s$ and $2p$ levels are R_s and R_p, respectively, then for cw laser excitation of the $2s_{1/2}$-$2p_{3/2}$ transition [19]

$$\frac{\Delta\Gamma}{\Gamma}=\frac{\left(\frac{I_0}{I_{\rm sat}}\right)\left(\frac{R_s}{R_p}\right)\left(\frac{\gamma_p}{2}\right)^2}{(\omega-\omega_0)^2+\left(\frac{\gamma_p}{2}\right)^2\left(1+\frac{I_0}{I_{\rm sat}}\right)}, \tag{1}$$

where ω_0 is the resonance frequency and γ_s and γ_p are decay rates of the $2s$ and the $2p$, respectively. I_0 is the laser intensity and the quantity $I_{\rm sat}$ is the saturation intensity given by

$$I_{\rm sat}=\frac{Z^2\gamma_p\gamma_s\hbar}{48\pi\alpha a_0^2}, \tag{2}$$

where α is the fine-structure constant, a_0 is the Bohr radius, and Z is the nuclear charge. At 1.5 keV the ratio of electron-impact excitation rates of the $2s_{1/2}$ and $2p$ states $R_S/R_P \approx 1/8$ [32].

Due to the strong electrostatic field in the trap caused by the space charge of the electron beam, the Stark-quenched decay rate of the $2s_{1/2}$ state [33] has to be considered for γ_s in Eq. (1). For an electron beam energy and current of 1.5 keV and 30 mA, the root-mean-square electric field averaged over the electron beam can be estimated to be 4.8×10^5 V/m. The motional electric field due to the motion of the ions in the 3-T field is estimated to be more than an order of magnitude smaller and this contribution should be negligible. The quenched decay rate of the $2s_{1/2}$ state can be described by [33,34]

$$\gamma_s'=\gamma_s+\frac{|V_{ps}|^2\gamma_p}{\hbar^2\left[\omega_{ps}^2+\left(\frac{\gamma_p^2}{4}\right)\right]}+\frac{|V_{qs}|^2\gamma_q}{\hbar^2\left[(\omega_{pq}-\omega_{ps})^2+\left(\frac{\gamma_p^2}{4}\right)\right]}, \tag{3}$$

where γ_s, γ_p, and γ_q are the natural decay rates of the unperturbed $2s_{1/2}$, $2p_{1/2}$, and $2p_{3/2}$ states, respectively, ω_{ps} is the Lamb shift, and ω_{pq} the fine-structure splitting. The second and third terms represent the decay rates induced by admixtures of the $2p_{1/2}$ and $2p_{3/2}$ states, respectively. V_{ps} and V_{qs} are the electric-dipole matrix elements between the appropriate two states in each case [28]. Making the approximation that the ion cloud of N^{6+} ions has a uniform density over the electron beam, Eq. (3) implies that the quenched decay rate of the $2s_{1/2}$ state is 2.8×10^6 s^{-1}. Using this value of γ_s', the saturation intensity given by Eq. (2) is about 7.3 W/mm^2, and the fractional change in Lyman-α at the resonance peak, with the intensity leveled at 1.15 W/mm^2, is estimated from Eq. (1) to be 1.7%. Allowing for unresolved x-ray backgrounds the predicted signal-to-background ratio is hence about 1%, in reasonable agreement with our observation, see Fig. 4(b). Possible reasons for the remaining discrepancy include incomplete dead-time correction in the

Si(Li) detector signal, nonoptimal alignment of the laser and electron beam, and unaccounted for backgrounds in the spectrum in Fig. 3(a).

The energy level shifts of $2s_{1/2}$, $2p_{1/2}$, and $2p_{3/2}$ states in a field 4.8×10^5 V/m due to the Stark effect are all less than 2×10^{-4} cm^{-1} and are negligible here. The effect on the resonance centroid due to saturation and the measured variation in the laser power is less than 0.1 cm^{-1}, well below the quoted error. The energy level shifts of the $M_J=\pm1/2$ substates of the $2s_{1/2}$, $2p_{1/2}$, and the $\pm1/2$ substates of the $2p_{3/2}$ due to the Zeeman effect in a magnetic field 3 T are ±1.4 cm^{-1}, ±0.49 cm^{-1}, and ±0.93 cm^{-1}, respectively, and broaden the line shape but produce negligible centroid shift. For our geometry, the energy splitting induced by the Zeeman effect is estimated to be 0.93 cm^{-1}, Eq. (1) implies a saturated width of 8.6 cm^{-1}, and the contribution to the resonance line width from Doppler broadening is estimated to be 0.13 cm^{-1}. This leads to a combined full width at half maximum of 8.8 cm^{-1}, consistent with the observed width. As regards the $2s_{1/2}$-$2p_{3/2}$ transition energy, the measured value 835.0 ± 0.5 cm^{-1} is in good agreement with Myers and Tarbutt's more accurate fast-beam experiment 834.94 ± 0.08 cm^{-1} [7] and Ivanov and Karshenboim's theory 834.928 ± 0.007 cm^{-1} [25].

In conclusion, an enhancement of Lyman-α radiation from hydrogenlike nitrogen ions trapped in an EBIT due to laser-induced excitation of the $2s_{1/2}$-$2p_{3/2}$ transition has been clearly observed, and an investigation of the wavelength dependence of this signal has been carried out.

This work was partially supported by the Japan Science and Technology Corporation, the EPSRC (UK), and the DTI under the NMS Quantum Metrology Program (Contract No. FQM1/A01). One of us (E.G.M) acknowledges support by NSF, Grant No. PHY-9970991; NATO CRG-960003; and the State of Florida. Technical support by Peter Hirst and Tony Handford (Oxford), and Jerry Hutchins, Kevin Kiley, and Ken Schaub (FSU), is greatly appreciated.

[1] H. W. Kugel and D. E. Murnick, Rep. Prog. Phys. **40**, 297 (1977).
[2] E. G. Myers, in *The Hydrogen Atom: Precision Physics of Simple Atomic Systems*, edited by S. G. Karshenboim *et al.* (Springer, New York, 2001), p. 179.
[3] P. J. Mohr, G. Plunien, and G. Soff, Phys. Rep. **293**, 227 (1998).
[4] M. I. Eides, H. Grotch, and V. A. Shelyuto, Phys. Rep. **342**, 63 (2001).
[5] J. Sapirstein, Rev. Mod. Phys. **70**, 55 (1998).
[6] I. Lindgren, Int. J. Quantum Chem. **57**, 683 (1996).
[7] E. G. Myers and M. R. Tarbutt, in *The Hydrogen Atom: Precision Physics of Simple Atomic Systems*, edited by S. G. Karshenboim *et al.* (Springer, New York, 2001), p. 688.
[8] H. W. Kugel, M. Leventhal, D. E. Murnick, C. K. N. Patel, and O. R. Wood, II, Phys. Rev. Lett. **35**, 647 (1975).
[9] P. Pellegrin, Y. El Masri, L. Palffy, and R. Prieels, Phys. Rev. Lett. **49**, 1762 (1982).
[10] H.-J. Pross, D. Budelsky, L. Kremer, D. Platte, P. von Brentano, J. Gassen, D. Muller, F. Scheuer, A. Pape, and J. C. Sens, Phys. Rev. A **48**, 1875 (1993).
[11] A. P. Georgiadis, D. Müller, H.-D. Sträter, J. Gassen, P. von Brentano, J. C. Sens, and A. Pape, Phys. Lett. A **115**, 108 (1986).
[12] O. R. Wood, II, C. K. N. Patel, D. E. Murnick, E. T. Nelson, M. Leventhal, H. W. Kugel, and Y. Niv, Phys. Rev. Lett. **48**, 398 (1982).
[13] M. Redshaw and E. G. Myers, Phys. Rev. Lett. **88**, 023002 (2002).
[14] I. Klaft *et al.*, Phys. Rev. Lett. **73**, 2425 (1994).
[15] P. Seelig *et al.*, Phys. Rev. Lett. **81**, 4824 (1998).
[16] J. K. Thompson, D. J. H. Howie, and E. G. Myers, Phys. Rev. A **57**, 180 (1998).
[17] M. A. Levine, R. E. Marrs, J. R. Henderson, D. A. Knapp, and M. B. Schneider, Phys. Scr., **T22**, 157 (1988).
[18] R. E. Marrs, S. R. Elliott, and D. A. Knapp, Phys. Rev. Lett. **72**, 4082 (1994).
[19] H. S. Margolis, D. Phil. thesis, University of Oxford, 1994 (unpublished).
[20] T. V. Back, H. S. Margolis, P. K. Oxley, J. D. Silver, and E. G. Myers, Hyperfine Interact. **114**, 203 (1998).
[21] L. Gruber, J. P. Holder, J. Steiger, B. R. Beck, H. E. DeWitt, J. Glassman, J. W. McDonald, D. A. Church, and D. Schneider, Phys. Rev. Lett. **86**, 636 (2001).
[22] D. Schneider, Hyperfine Interact. **99**, 47 (1996).
[23] D. A. Church *et al.*, in *Trapped Charged Particles and Fundamental Physics*, edited by Daniel H. E. Dubin and Dieter Schneider, AIP Conf. Proc. No. 457 (AIP, Woodbury, NY, 1999), p. 235.
[24] W. R. Johnson and G. Soff, At. Data Nucl. Data Tables **33**, 405 (1985).
[25] V. G. Ivanov and S. G. Karshenboim, in *The Hydrogen Atom: Precision Physics of Simple Atomic Systems*, edited by S. G. Karshenboim *et al.* (Springer, New York, 2001), p. 635.
[26] S. P. Goldman and G. W. F. Drake, Phys. Rev. A **24**, 183 (1981).
[27] S. P. Goldman, Phys. Rev. A **40**, 1185 (1989).
[28] M. Hillery and P. J. Mohr, Phys. Rev. A **21**, 24 (1980).
[29] J. D. Silver *et al.*, Rev. Sci. Instrum. **65**, 1072 (1994).
[30] Soft X-ray Window, AP1.4, supplied by Gresham Scientific Instruments Ltd.
[31] L. C. Bradley, K. L. SooHoo, and C. Freed, IEEE J. Quantum Electron. **22**, 234 (1986).
[32] J. Callaway, Phys. Lett. A **96**, 83 (1983).
[33] W. E. Lamb, Jr. and R. C. Retherford, Phys. Rev. **79**, 549 (1950).
[34] V. Zacek, H. Bohn, H. Brum, T. Faestermann, F. v. Feilitzsch, G. Giorginis, P. Kienle, and S. Schuhbeck, Z. Phys. A **318**, 7 (1984).